

Microglial production of quinolinic acid as a target and a biomarker of the antidepressant effect of ketamine

Franck Verdonk, Anne-Cécile Petit, Pierre Abdel-Ahad, Fabien Vinckier, Gregory Jouvion, Pierre de Maricourt, Gabriela Ferreira de Medeiros, Anne Danckaert, Juliette van Steenwinckel, Michael Blatzer, et al.

▶ **To cite this version:**

Franck Verdonk, Anne-Cécile Petit, Pierre Abdel-Ahad, Fabien Vinckier, Gregory Jouvion, et al.. Microglial production of quinolinic acid as a target and a biomarker of the antidepressant effect of ketamine. Brain, Behavior, and Immunity, 2019, 81, pp.361 - 373. 10.1016/j.bbi.2019.06.033 . pasteur-03263257

HAL Id: pasteur-03263257

https://pasteur.hal.science/pasteur-03263257

Submitted on 17 Jun 2021

HAL is a multi-disciplinary open access archive for the deposit and dissemination of scientific research documents, whether they are published or not. The documents may come from teaching and research institutions in France or abroad, or from public or private research centers.

L'archive ouverte pluridisciplinaire **HAL**, est destinée au dépôt et à la diffusion de documents scientifiques de niveau recherche, publiés ou non, émanant des établissements d'enseignement et de recherche français ou étrangers, des laboratoires publics ou privés.



Distributed under a Creative Commons Attribution - NonCommercial - NoDerivatives 4.0 International License

Brain, Behavior, and Immunity 81 (2019) 361–373

Contents lists available at ScienceDirect

Brain, Behavior, and Immunity

journal homepage: www.elsevier.com/locate/ybrbi

Microglial production of quinolinic acid as a target and a biomarker of the antidepressant effect of ketamine

Franck Verdonk[a,b,c], Anne-Cécile Petit[a,d,e], Pierre Abdel-Ahad[d,e,f], Fabien Vinckier[d,e,f], Gregory Jouvion[a], Pierre de Maricourt[d,e,f], Gabriela Ferreira De Medeiros[a], Anne Danckaert[a,g], Juliette Van Steenwinckel[h,i], Michael Blatzer[a], Anna Maignan[j], Olivier Langeron[a,c,k], Tarek Sharshar[a,e,l], Jacques Callebert[m], Jean-Marie Launay[m], Fabrice Chrétien[a,e,n,*], Raphael Gaillard[a,d,e,*]

[a] Institut Pasteur, Experimental Neuropathology Unit, Infection and Epidemiology Department, Paris, France
[b] Department of Anaesthesiology and Intensive Care, Saint Antoine Hospital, Assistance Publique-Hôpitaux de Paris, Paris, France
[c] Sorbonne University, Paris, France
[d] Service Hospitalo Universitaire, Centre Hospitalier Sainte-Anne, Paris, France
[e] Paris Descartes University, Sorbonne Paris Cité, Paris, France
[f] INSERM, Laboratoire de "Physiopathologie des maladies Psychiatriques", Centre de psychiatrie et neurosciences, CPN U894, Institut de psychiatrie (GDR 3557), Paris, France
[g] Institut Pasteur, UtechS Photonic BioImaging (Imagopole) – C2RT, Paris, France
[h] Inserm, U1141 Paris, France
[i] Paris Diderot University, Sorbonne Paris Cité, UMRS 1141, F-75019 Paris, France
[j] Service Universitaire de Psychiatrie d'adultes, Centre Hospitalier de Versailles, Le Chesnay, France
[k] Multidisciplinary Intensive Care Unit, Department of Anesthesiology and Critical Care, La Pitié-Salpêtrière Hospital, Assistance Publique-Hôpitaux de Paris, Paris, France
[l] Department of Intensive Care, Centre Hospitalier Sainte Anne, Paris, France
[m] Service de Biochimie et Biologie Moléculaire, INSERM U942, Hôpital Lariboisière, Assistance Publique-Hôpitaux de Paris, Paris, France
[n] Laboratoire hospitalo-universitaire de Neuropathologie, Centre Hospitalier Sainte Anne, Paris, France

ARTICLE INFO

Keywords:
Depression
Ketamine
Inflammation
Microglia
Murine model
Translational research
Quinolinic acid
Biomarker

ABSTRACT

Major depressive disorder is a complex multifactorial condition with a so far poorly characterized underlying pathophysiology. Consequently, the available treatments are far from satisfactory as it is estimated that up to 30% of patients are resistant to conventional treatment. Recent comprehensive evidence has been accumulated which suggests that inflammation may be implied in the etiology of this disease. Here we investigated ketamine as an innovative treatment strategy due to its immune-modulating capacities. In a murine model of LPS-induced depressive-like behavior we demonstrated that a single dose of ketamine restores the LPS-induced depressive-like alterations. These behavioral effects are associated with i/ a reversal of anxiety and reduced self-care, ii/ a decrease in parenchymal cytokine production, iii/ a modulation of the microglial reactivity and iv/ a decrease in microglial quinolinic acid production that is correlated with plasmatic peripheral production. In a translational approach, we show that kynurenic acid to quinolinic acid ratio is a predictor of ketamine response in treatment-resistant depressed patients and that the reduction in quinolinic acid after a ketamine infusion is a predictor of the reduction in MADRS score. Our results suggest that microglia is a key therapeutic target and that quinolinic acid is a biomarker of ketamine response in major depressive disorder.

1. Introduction

Major depressive disorder is considered one of the ten leading causes of disability worldwide (Langlieb and Guico-Pabia, 2010). Nevertheless, current antidepressant therapies targeting primarily monoaminergic neurotransmission systems have been found to be insufficient. Remission rates are lower than 30% at each treatment line with a cumulative remission rate lower than 65% (Sinyor et al., 2010).

This insufficient efficacy may be attributed to a poorly understood pathophysiology of depressive disorders. The monoaminergic neuronal

* Corresponding authors at: Institut Pasteur, 28 rue du Docteur Roux, 75015 Paris, France.
E-mail addresses: fabrice.chretien@pasteur.fr (F. Chrétien), raphael.gaillard@normalesup.org (R. Gaillard).

https://doi.org/10.1016/j.bbi.2019.06.033
Received 27 April 2019; Received in revised form 21 June 2019; Accepted 22 June 2019
Available online 28 June 2019
0889-1591/ © 2019 The Authors. Published by Elsevier Inc. This is an open access article under the CC BY-NC-ND license (http://creativecommons.org/licenses/BY-NC-ND/4.0/).

dysfunctions have been extensively studied in depressed patients (Zanos and Gould, 2018). However, other pathophysiological mechanisms are known to be implied in depression, such as neuroinflammation (Kiecolt-Glaser et al., 2015). Several post-mortem studies have reported an increased expression of interleukin-1 β (IL-1β), IL-6, tumor necrosis factor (TNF) and Toll-like receptors 3 and 4 (TLR3 and TLR4) in the brains of depressed patients (Maes, 1999; Miller et al., 2009). Moreover, plasma levels of IL-1β, IL-6, TNF and C-reactive protein (CRP) appear to be potentially appropriate inflammatory biomarkers in depressed patients (Miller et al., 2009). Furthermore, the administration of pro-inflammatory cytokines (e.g. interferon-α (IFN-α)) or their inducers (e.g. endotoxin, typhoid vaccine) produced symptoms of depression in individuals without psychiatric diseases (Bonaccorso et al., 2002; Capuron et al., 2002), demonstrating a causal role of inflammation in at least a subcategory of major depressive disorders (Kappelmann et al., 2018). Depression-related neuroinflammation can divert tryptophan metabolism toward the kynurenine pathway, leading to a decrease in serotonin synthesis and to the production of quinolinic acid, acting on glutamate transmission as an N-Methyl-D-Aspartate (NMDA) receptor agonist (Dantzer et al., 2011; Raison et al., 2013). Several studies reported that quinolinic acid and kynurenic acid blood levels are correlated with depression score in patients with major depressive disorder (Liu et al., 2018; Ogyu et al., 2018). Moreover, in a post-mortem study, the density of microglial cells producing quinolinic acid appears to be increased in anterior cingulate gyrus of depressed suicidal patients (Steiner et al., 2011).

In this context, ketamine, an anesthetic drug and powerful analgesic, is a very promising molecule. It has been repeatedly tested as an innovative antidepressant drug over the past ten years (Berman et al., 2000). It has an exciting therapeutic potential with rapid-onset and impressive efficacy in patients with treatment-resistant depression (Zarate et al., 2006). Indeed it acts as a non-competitive glutamate NMDA receptor antagonist, which induces the activation of intracellular signaling proteins (mTOR, GSK3) and the synthesis of new synaptic proteins (Duman et al., 2012). In a recent study, Walker et al. demonstrated a behavioral improvement induced by ketamine in a mouse model of LPS-induced depression with no biological correlate of this behavioral effect (Walker et al., 2013). The hypothesis retained for the mechanism underlying the antidepressant effect of ketamine was its NMDA antagonism, which could counteract quinolinic acid accumulation (Dantzer et al., 2011).

Ketamine also has anti-inflammatory properties and inhibits the systemic production of pro-inflammatory cytokines (Beilin et al., 2007). Numerous *in vitro* studies have highlighted that ketamine, in inflammatory conditions, reduces the production of HMGB-1 (Tan et al., 2015), IL6 or TNF alpha through the suppression of the TLR4-mediated pathway (Wu et al., 2008) and induces changes in microglial cells (Chang et al., 2009). Furthermore, experimental animal models and human post-mortem studies have demonstrated an association between depressive behavior and microglial activation and between the reversibility of the induced depressive behavior and microglial changes (Yirmiya et al., 2015). However microglial changes as a potential direct target of ketamine explaining its antidepressant effect had thus far not been studied.

We therefore aimed to investigate the effects of ketamine on a well-documented murine model of depression induced by LPS systemic infusion with extensive measurements of microglial activity. Consecutively, based on the results obtained with this approach, we explored a potential marker of efficacy in patients with treatment-resistant depression treated with repeated infusions of ketamine.

2. Materials and methods

2.1. Preclinical study

2.1.1. Animal modeling

All animals used in the study were between 9 and 11 weeks old. The mice were housed in cages in groups of 7, at 22 ± 1.5 °C in a humidity-controlled environment, with a 12 h light/dark cycle. Food and water were available *ad libitum* in accordance with international guidelines. The experiments were performed on wild-type C57BL/6JRj male mice purchased from Janvier Laboratory and in-house knock-in CX3CR1$^{GFP/+}$ male mice. In these mice, green fluorescent protein (GFP) reporter gene is under the control of the fractalkine receptor (CX3CR1) promoter. The expression of GFP gene is constitutively turned on in microglial cells, which allowed us to image them selectively without any immunochemistry method that could be deleterious for the integrity of the tissue and cell morphology (Jung et al., 2000). The C57BL/6JRj mice were used to investigate the microglial phenotype by qRT-PCR. All other experiments were performed with the knock-in CX3CR1$^{GFP/+}$ mice.

2.1.2. Ethical protocol

All experimental protocols were approved by the Ethics Committee of the Institut Pasteur (CETEA, 2015-0038) and the Ministry of National Education and Research (APAFIS#6449-2016052515127983 v1).

2.1.3. Pharmacological intervention

Experimental groups (n = 12–16 mice per group) were designed as followed: two conditions were used: control (CTRL)/lipopolysaccharide (LPS) with different treatments: placebo (PLACEBO)/ketamine at 90 mg/kg (KET90)/ketamine at 10 mg/kg (KET10).

The mice included in the control condition received an intraperitoneal (IP) injection of 100 µL of isotonic saline solution (NaCl 0.9%) and those included in the LPS condition received a LPS IP injection (Sigma Aldrich® E. coli 0111:B4, Lot 095M4165V) at a dose of 1 mg/kg (diluted in isotonic saline solution). Immediately after this injection, which defined the condition, the treatments were administrated. They consisted respectively of an intraperitoneal (IP) injection of 100 µL of isotonic saline solution (NaCl 0.9%) or of ketamine at a dose of 90 mg/kg or at 10 mg/kg (Imalgen® 1000, MERIAL, diluted in isotonic saline solution). At the end, five groups were compared: CTRL-PLACEBO, CTRL-KET90, LPS-PLACEBO, LPS-KET90 and LPS-KET10. The dose of LPS (1 mg/kg) was chosen for its ability to induce depressive-like behaviors in mice (O'Connor et al., 2009). Ketamine dose of 90 mg/kg was chosen as a positive control for the effect of ketamine on the function of innate immune cells (Takahashi et al., 2010) and the dose of 10 mg/kg for its ability to have antidepressant-like activity in mice (Walker et al., 2013) and to compare the effects observed in mice to the effects obtained in patients treated with infusions of low doses of ketamine.

Mice from both experiments were euthanized by cervical dislocation 32 h after the pharmacological intervention for brain collection (Fig. 1a) allowing performing two distinct behavioral tests in a 6 h interval. Cervical dislocation was authorized by the Ethics Committee of the Institut Pasteur and the French Ministry of National Education and Research in order to avoid any molecular interaction with any type of anesthesia or with carbon dioxide before brain analysis.

2.1.4. Behavioral testing

The same cohort of animals was subjected to two different behavioral tests, one testing anxiety-like behavior and the other testing self-care, both features present in experimental models of depression (David et al., 2009). Acute treatment with ketamine is known to reduce latency to feed in NSF and to increase grooming in ST (Ma et al., 2017; Pham et al., 2017; Ramaker and Dulawa, 2017). Thus twenty four hours after the pharmacological intervention, each animal was tested successively in the *Novelty Suppressed Feeding Test* (NSF) (Mendez-David et al., 2014) and then in the *Splash Test* (ST) (David et al., 2009), with a 6 h interval between both tests (see Suppl. Material and Methods for details). All behavioral tests took place during the light phase of the light/dark cycle.

2.1.5. Tissue preparation

After euthanasia by cervical dislocation, the brains were immediately removed and sectioned along the inter-hemispherical fissure on a sagittal plane. The left hemisphere, dedicated to the morphological

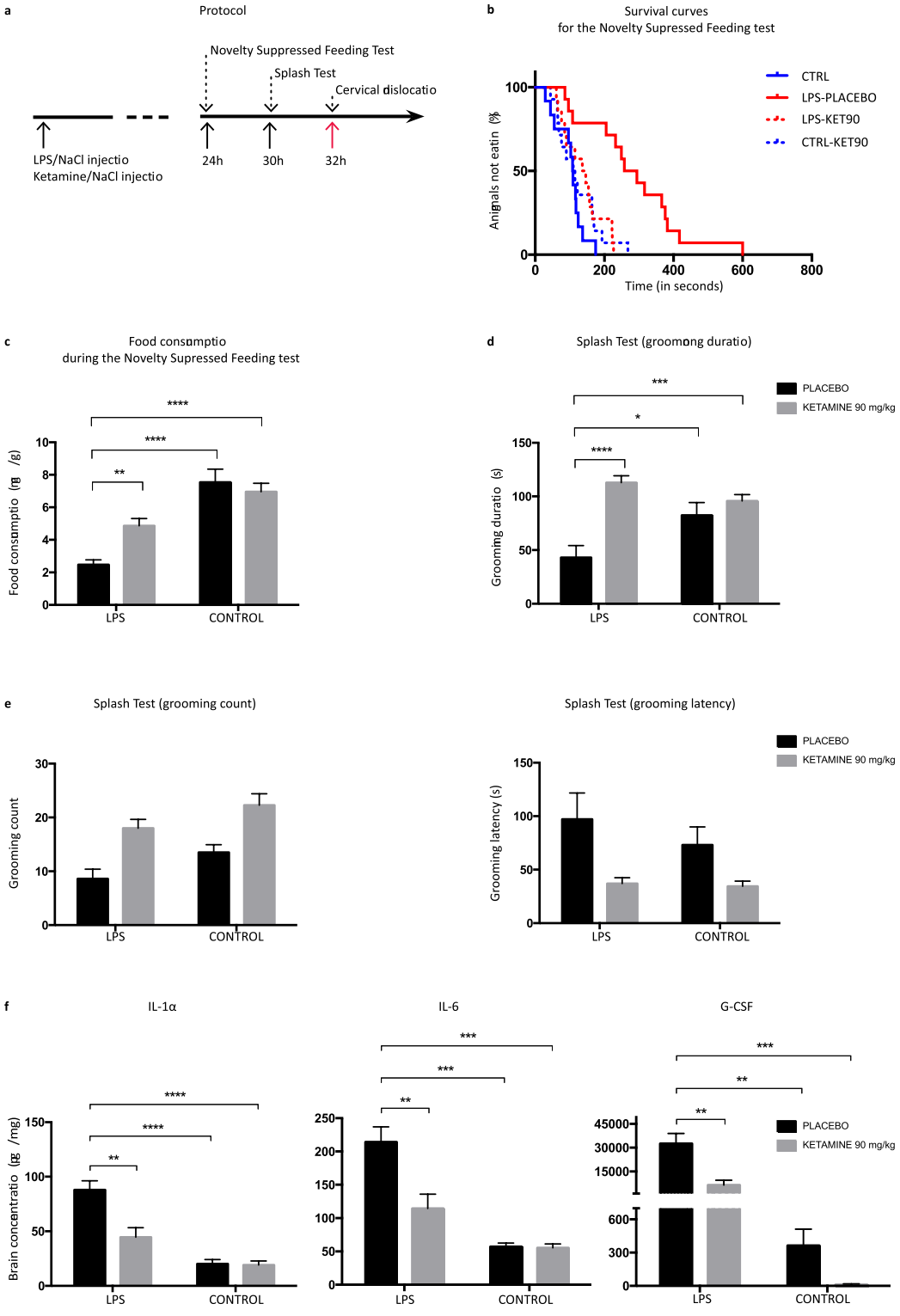


Fig. 1. Ketamine abrogates lipopolysaccharide (LPS)-induced depressive-like behavior and pro-inflammatory cytokine production in the brain parenchyma. (a) Diagram of the experimental set-up and procedure the murine model. (b) Survival curve of the latency before feeding after 24 h in seconds for mice of the different groups (n = 10–12 per group). (c) Mean food consumption during the NSF (mg/g of mouse). (d) Grooming duration in seconds during the Splash Test (n = 10–12 per group). (e) Grooming count and grooming latency in seconds during the Splash Test (n = 10–12 per group). (f) Representative results of Luminex assays of interleukin-1α (IL-1 α), interleukin-6 (IL-6) and granulocyte-colony-stimulating factor (G-CSF) are shown 32 h after LPS injection, depicted as the mean values of protein expression in pg/mg in cerebral tissue of six mice per group (n = 6 mice per group). Data shown are median values (± SEM). Gray bars represent ketamine-treated mice from either LPS or Control groups, and black bars represent placebo-treated mice from either LPS or Control groups. Two-way analyses of variance (ANOVAs) (LPS *vs* NaCl × ketamine *vs* placebo) were performed. When a significant interaction was observed, planned comparisons were performed for the LPS/Placebo group against the three other groups. The significance of these planned comparisons is indicated with asterisks ($^{*}p < 0.05$, $^{**}p < 0.01$, $^{***}p < 0.001$, $^{****}p < 0.0001$).

analysis, was fixed for 24 h in a 4% paraformaldehyde solution (QPath®, VWR Chemicals, Fontenay Sous Bois, France) and then stored in a 0.1% paraformaldehyde solution until carrying out floating sections of 80 µm along a sagittal plane using a vibratome (VT 1000 S, Leica®, Germany). The most medial section was then used for the morphological analysis. The right cerebral hemisphere was either frozen in liquid nitrogen and stored at −80° in order to later quantify cytokine and chemokine concentrations via Luminex® assays and metabolites of the kynurenine pathway by high-performance liquid chromatography (HPLC) or was immediately dedicated to microglial isolation by magnetic-activated cell sorting.

2.1.6. *Luminex ® assays*

The frozen brain samples were weighed and then placed in 500 µL of isotonic saline solution in Lysing Matrix tubes (Lysing Matrix Z 2 mL Tubes, MP Biomedicals ®) before being lysed using a FastPrep system. Samples were then centrifuged and the supernatant was aliquoted and processed for multiple cytokine and chemokine analysis using the

Luminex® flow cytometry technique (Magnetic Luminex Screening Assays, R&D Systems®, LXSAMSM-13). The cytokines screened are cited in Suppl. Material and Methods.

2.1.7. Microglial morphology imaging and analysis

Microglial morphologic criteria were determined with an automated confocal tissue imaging system coupled to morphological modelling in $CX3CR1^{GFP/+}$ transgenic mice. This analysis was performed on sagittal cerebral floating sections of the left hemisphere placed on glass slides with FluoroMount (FluoroMount-G Mounting Medium, FluoProbes).

The image acquisition was carried out according to a previously validated protocol (Verdonk et al., 2016) using a confocal spinning disk microscope (Cell Voyager – CV1000, Yokogawa®, Japan) equipped with a UPLSAPO objective 40x/NA 0.9. More details are available in Suppl. Material and Methods.

An automatic analysis was applied using an analysis script developed with the image analysis software Acapella™ (version 2.7 – Perkin Elmer Technologies, Waltham, USA). The following morphological criteria have been defined for each microglial cell on more than 3000 microglial cells by group: the area of the cell body and the cytoplasmic area, defined as the area of the cytoplasm included in the primary branches, expressed in μm^2; a second set of calculated criteria extrapolated from the previous ones yielded the complexity index (CI) and the covered environment area (CEA). First, we defined the CI by the ratio between the number of segments of each ramification of each cell multiplied by the sum of the nodes on one hand and the number of primary branches on the other hand. Thus we obtained an average complexity relative to the number of primary branches for each microglial cell.

$$CI = \frac{nb\ of\ segments \times (nb\ of\ nodes\ 1 + nb\ of\ nodes\ 2)}{nb\ of\ roots}$$

On the other hand, CEA represents the 2D total surface covered by its ramifications and defined as the area of the polygon formed by linking the extremities of its processes, expressed in μm^2

2.1.8. Isolation of murine microglial cells CD11b+ using magnetic-activated cell sorting (MACS)

The magnetic-activated cell sorting method (MACS® Technology), following the protocol suggested by Miltenyi Biotec® and described in Suppl. Material and Methods, was used for isolation of microglia cells with positive selection with the magnetic microbeads coupled to anti-CD11b antibodies.

2.1.9. Reverse transcribed–quantitative PCR (RT-qPCR)

Total RNA was isolated from microglial cells using the RNAeasy Micro kit (Qiagen). The complementary DNA synthesis was performed with the Superscript II Reverse transcriptase (Company). RT-qPCR was performed using Power Sybr Green PCR Master Mix (Applied Biosystems®) on the StepOne™ Plus RealTime PCR system (Applied Biosystems). Data were analyzed using StepOne Plus RT PCR software v2.1 and Microsoft Excel.

Expression levels were calculated with the 2-ΔΔCT method using the TATA-Binding Protein (TBP) gene as housekeeper (Schmittgen and Livak, 2008).

To choose the genes of interest, we adopted the nomenclature described in published works (Chhor et al., 2013; Colton, 2009; Mantovani et al., 2004; Ransohoff and Perry, 2009) to define the microglial phenotype (M1, M2a or M2b) (see Suppl. Material and Methods for details). We also included the expression of the hemoxygenase-1 gene (HO-1).

2.1.10. Tryptophan catabolite measurements

Cerebral and plasmatic levels of tryptophan (TRYP), serotonin (5HT), kynurenine (KYN), 5-hydroxyindoleacetic acid (5-HIAA), 3-hydroxykynurénine (3HK), kynurenic acid (KYNA) and quinolinic acid (QUIN) were measured using high-performance liquid chromatography (HPLC) as described by Fujigaki et al. (2003) (see Suppl. Material and Methods for details).

2.1.11. Statistical data analysis

Prism 6.0 (GraphPad Software Inc.©, USA) was used for the statistical analysis. Two types of complementary approaches were examined using and comparing two different concentrations of ketamine, an anesthetic dose, 90 mg/kg, and a sub-anesthetic dose, 10 mg/kg. First, two-way analyses of variances (ANOVAs) (LPS *vs* control × ketamine at 90 mg/kg *vs* placebo) were performed for all measurements of biochemistry and cellular analysis or of the readout of depressive-like behavior parameters. Significant differences between groups were further evaluated using Tukey's post hoc tests. In order to remain focused on the study of a specific effect of ketamine on our inflammatory model of depression, the interpretation of the tests focusses only on significant interactions. Positive analyses which were specific to the condition or treatment criteria will not be addressed here. Second, after confirmation of a significant interaction we assessed a potential dose effect by comparing the doses of 10 mg/kg (LPS-KET10) and 90 mg/kg (LPS-KET90) in the LPS induced depressive behavior (LPS-PLACEBO). The data were analyzed using the Kruskal-Wallis test after being assessed for non-normal distribution. The alpha level of 0.05 was adjusted for the number of comparisons to control for family-wise error. Only significant comparisons between groups are indicated in the figures. When multiple comparisons were needed, analysis using Sidak's or Dunn's corrections were realized.

Comparisons for tryptophan catabolite levels between plasma and brain were performed using Spearman's rank correlation coefficients after assessment of non-normally distribution of these levels.

2.2. Clinical study

2.2.1. Patients and study design

In an observational cohort pilot study, 15 in-patients hospitalized at Sainte-Anne Hospital (Paris), suffering from a major depressive episode (unipolar or bipolar) according to DSM-5 criteria, and eligible for ketamine treatment based on the resistance of the depressive episode were included. Patients with DSM-5 schizophrenia spectrum disorder, neurodevelopmental disorders and neurocognitive disorders were excluded. All patients gave their written informed consent for inclusion. The present investigation was conducted in accordance with the ethical standards and according to the Declaration of Helsinki, and was approved by the local ethics committee (#AAA-2018-08009).

Ketamine treatment was administered intravenously over forty minutes at a dose of 0.5 mg/kg. The frequency of administration (one or two times per week), the total number of infusions during a cycle of ketamine treatment and the co-prescribed medications were decided by the patient's psychiatrist in naturalistic conditions (see Table 4 for details).

Before and after each infusion, depressive symptoms were assessed and blood samples were collected to perform HPLC and mass fragmentography measures of tryptophan catabolites in plasma (see Suppl. Material and Methods for details). Blood samples of 15 age and sex-matched healthy controls were also analyzed. These samples were collected from orthopedic patients without comorbidity following cast removal.

2.2.2. Statistical analysis

Comparisons for biological parameters between patients and controls were performed using Wilcoxon signed rank test to compare non-normally distributed parameters and unpaired *t*-test for normally distributed parameters.

Two sets of analyses were performed. First, we investigated the whole cycle of ketamine treatment, meaning the difference between the

Table 1
Ketamine abrogates pro-inflammatory cytokine production in the brain parenchyma.

	LPS-PLACEBO	LPS-KET90	CTRL-PLACEBO	CTRL-KET90	Interaction	Condition	Treatment
IL-1α	88.06	37.75	15.26	15.13	**0.0281**	< 0.0001	0.0217
IL-1β	804.1	719.9	655.4	1117	NS	NS	NS
IL-2	31.87	31.69	33.03	43.59	NS	NS	NS
IL-3	32.98	28.56	24.77	26.47	NS	NS	NS
IL-5	25.78	24.32	20.34	29.75	NS	NS	NS
IL-6	209.2	80.57	53.71	59.75	**0.0485**	< 0.0001	0.0411
IL-9	153.4	796.3	616.3	1221	NS	0.0008	< 0.0001
IL-10	93.29	62.54	50.18	64.02	NS	NS	0.0298
IL-12(p40)	657.6	341.4	82.23	52.44	NS	NS	NS
IL-12(p70)	546.2	504.4	439.4	612.2	NS	NS	NS
IL-13	914.5	861.6	806.6	1006	NS	NS	NS
IL-17	59.33	61.21	51.57	79.41	NS	NS	NS
Eotaxin	1994	1807	1208	3375	**0.0476**	NS	NS
G-CSF	29036	1607	249.6	0	**0.0304**	0.0019	0.0264
GM-CSF	254.6	216.8	203.7	0	NS	NS	NS
IFN-g	73.08	69.97	59.77	88.61	NS	NS	0.0173
KC	1147	342.1	62.36	79.11	NS	NS	NS
MCP1	945.4	638.3	235	361.4	NS	< 0.0001	NS
MIP1a	413.1	352.6	255.8	360.6	NS	0.0141	NS
MIP1b	153.8	142.4	119.8	226.6	**0.0496**	NS	0.0316
RANTES	94.08	48.07	29.76	29.52	NS	0.023	NS
TNFα	3881	4022	3088	5790	**0.0442**	NS	0.0253
FGFβ	3266	2804	1889	1927	NS	< 0.0001	NS
MIG	1433	1169	1077	995.1	NS	NS	NS
VEGF	79.82	113	116.4	134	NS	0.0012	NS

The data shown represent median values of Luminex assays (n = 6 mice per group). Two-way analyses of variance (ANOVAs) (LPS *vs* NaCl × ketamine *vs* placebo) were performed. The "interaction" column indicates if an interaction between the condition (LPS or control) and the treatment (ketamine or placebo) could affect the results, the "condition" and "treatment" columns indicate if the condition (LPS or control) or the treatment (ketamine or placebo) could affect the results. NS: not significant.

initial evaluation before the first ketamine infusion and the final evaluation, 24 h after the last ketamine infusion; n = 15 (see Suppl. Material and Methods for details). Second, as the ketamine effect on depressive symptoms is known to be very rapid (Zarate et al., 2006) *ie* within the 24 h following the infusion, we evaluated the changes of clinical and biological variables around each infusion (pre- and post-infusion). We pooled all infusions of all patients; n = 83 after excluding missing data points (see Suppl. Material and Methods for details).

3. Results

3.1. Preclinical study

Two types of complementary approaches were examined using and comparing two different concentrations of ketamine, an anesthetic dose, 90 mg/kg and a sub-anesthetic dose, 10 mg/kg, mainly used in the field of depressive-like behavior in animal experiments. First, two-way analyses of variances (ANOVAs) (LPS *vs* control × ketamine at 90 mg/kg *vs* placebo) were performed. After confirming a significant interaction, we assessed a potential dose effect by comparing the doses of 10 mg/kg (LPS-KET10) and 90 mg/kg (LPS-KET90) in the LPS induced depressive behavior (LPS-PLACEBO).

Before assessing tissular and microglial effects of ketamine, we confirmed that ketamine restores LPS-induced depressive-like behavior in our model. The Novelty Suppressed Feeding test (NSF) (Fig. 1b and c) and the Splash Test (ST) (Fig. 1d and e) confirmed a positive effect of ketamine with significant LPS *vs* control × ketamine *vs* placebo interactions (see Suppl. Data for details).

3.1.1. Investigating the effects of ketamine on the tissue: ketamine counteracts the LPS-induced pro-inflammatory cytokine release in the brain

A significant LPS *vs* control × ketamine *vs* placebo interaction is observed for IL-1α, IL-6, TNFα and G-CSF brain concentrations ($F(1,30) = 5.323$, $p = 0.0281$; $F(1,30) = 4.230$, $p = 0.0485$; $F(1,30) = 4.410$, $p = 0.0442$ and $F(1,30) = 5.166$, $p = 0.0304$ respectively). LPS alone induced a significant increase in the cerebral concentration of these cytokines in comparison with the CTRL-PLACEBO group (mean difference for IL-1α: 68 pg/mg, $p < 0.0001$; IL-6: 34 pg/mg, $p < 0.0001$; G-CSF: 32 μg/mg, $p = 0.002$). Ketamine administration reversed this enhanced cytokine production except for TNFα: the LPS-KET90 group presented with a significantly lower concentration than the LPS-PLACEBO group (mean difference = 43 pg/mg, $p = 0.0015$; 99 pg/mg, $p = 0.0028$ and 26 μg/mg, $p = 0.001$ respectively). These results indicate that these LPS-induced increase of pro-inflammatory cytokines and chemokine production in the brain were alleviated by ketamine administration. The LPS-KET90 group did not differ significantly from the CTRL-PLACEBO group (Fig. 1f). All chemokine and cytokine concentrations are available in Table 1.

In the LPS condition, mice receiving ketamine treatment at 10 mg/kg mirrored the cytokine profile of mice treated with 90 mg/kg (Table S1).

3.1.2. Investigating the effect of ketamine on the brain immune cells – microglia

3.1.2.1. LPS-induced morphological microglial reactivity was attenuated by ketamine. The morphology of the microglial cells in the prefrontal cortex and the hippocampus was studied in the $CX3CR1^{GFP/+}$ mice. The $CX3CR1^{GFP/+}$ mice presented a constant intensity of the GFP fluorescence regardless of the brain region.

In the prefrontal cortex, ketamine had a significant impact on the cell body area in combination with LPS as observed with a positive LPS *vs* control × ketamine *vs* placebo interaction ($F(1,19) = 4.59$, $p = 0.0453$). The LPS-PLACEBO group presented significantly higher microglial cell body areas in comparison to the CTRL-PLACEBO group as microglial activation marker (mean difference 3.6 μm^2, $p < 0.0001$). This effect was alleviated by ketamine. We observed a significant LPS *vs* control × ketamine *vs* placebo interaction for the cell complexity ($F(1,19) = 4.629$, $p = 0.0445$), but not for the cell environment area. Importantly, ketamine alone did not alter the cell body area or the complexity. (Fig. 2a and b). These interactions are not observed in the hippocampus (Fig. 2c).

In LPS condition, a lower ketamine dose (10 mg/kg) induced the

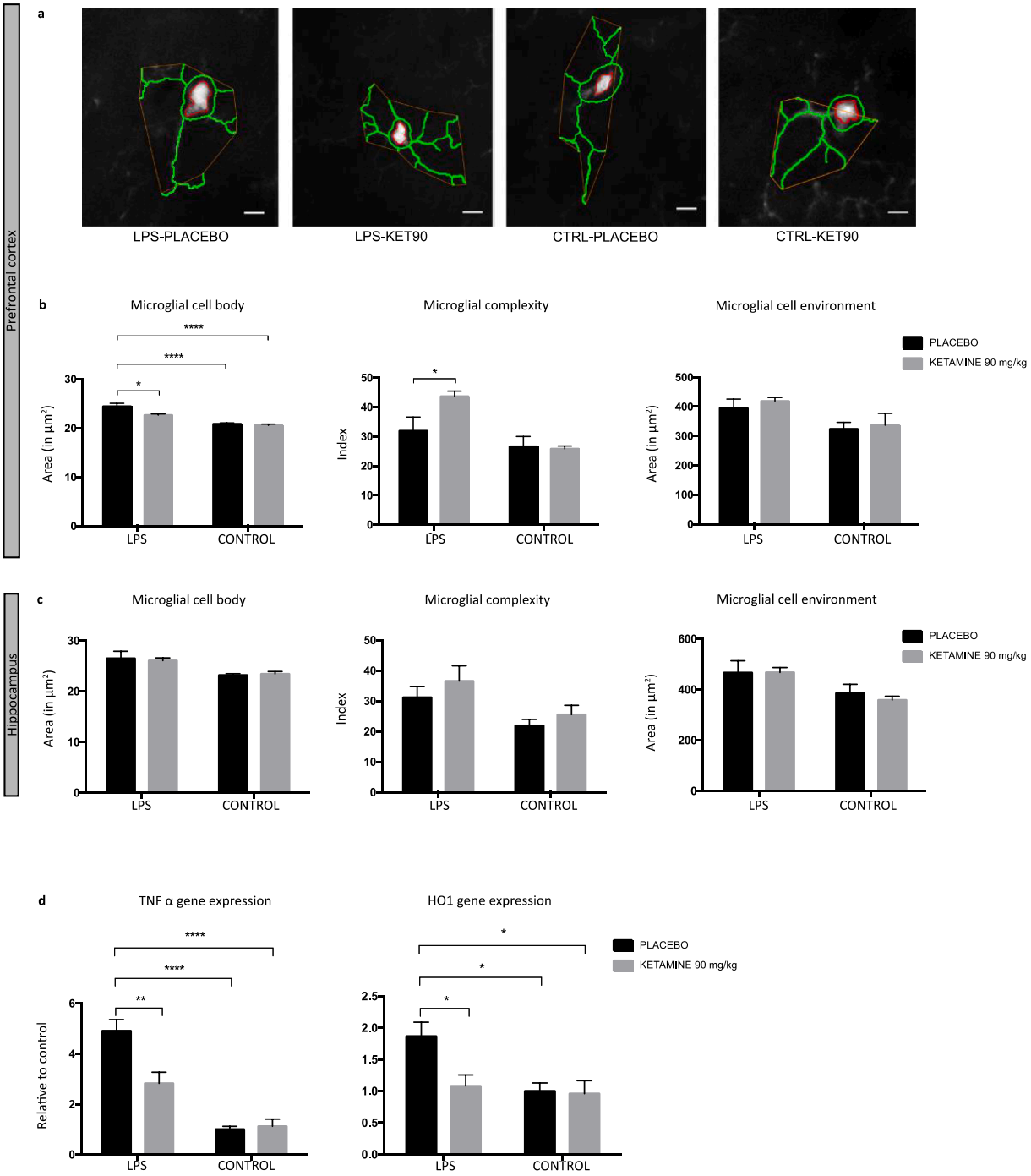


Fig. 2. Ketamine decreased microglial activation in the prefrontal cortex and induced neuroprotective mediator transcription. Microglial morphology was characterized using the following parameters: microglial cell body area, microglial complexity index and the microglial cell environment (the calculated criteria were extrapolated using the Acapella™ script). In CX3CR1$^{GFP/+}$ mice, 150 to 550 microglial cells were analyzed by region and by animal (n = 6 animals by group). (a) Morphological criteria characterizing a representative microglial cell. Cell body detection (red) was performed as starting point to characterize a microglial cell. The complexity index (green) and the covered environment area (CEA in orange) were deduced from ramification detection. Scale bar equals 10 µm. The cell body and the cell environment area (CEA) are expressed in µm^2 for the prefrontal cortex (b) and the hippocampus (c). (d) The data shown represent median values as fold changes using the $2^{-\Delta\Delta CT}$ method of TNF-α and HO1 gene expression in microglia relative to the control group (CTRL). (n = 6 mice per group). The data shown are median values (± SEM). Gray bars represent ketamine-treated mice from either LPS or Control groups, and black bars represent placebo-treated mice from either LPS or Control groups. Two-way analyses of variance (ANOVAs) (LPS *vs* NaCl × ketamine *vs* placebo) were performed. When a significant interaction was observed, planned comparisons were performed for the LPS/Placebo group against the three other groups. The significance of these planned comparisons is indicated with asterisks ($^{*}p < 0.05$, $^{**}p < 0.01$, $^{***}p < 0.001$, $^{****}p < 0.0001$).

same trends but without any statistical significance (Fig. S2a and b).

3.1.2.2. LPS induced cytotoxic microglia polarization while ketamine induced neuroprotective mediators (Table 2). During inflammation, microglia can produce either cytotoxic (M1 or M2b phenotype) or neuroprotective mediators (M2a).

Regarding the M1 phenotypic markers of extracted microglial cells, a significant LPS *vs* control × ketamine *vs* placebo interaction was

Table 2
Gene expression profiles of microglial phenotype markers relative to control group.

Phenotype	CTRL	LPS	KET90	LKET90	Interaction	Condition	Treatment
M1 phenotype							
CD32	1.025	1.35	0.695	1.97	NS	0.0024	NS
CD86	1.09	1.07	0.905	1.2	NS	NS	NS
Ptgs2	0.925	3.96	0.98	1.92	**0.0032**	< 0.0001	0.0102
M2a phenotype							
Lgals3	0.945	4.83	1.05	6.23	**0.0463**	< 0.0001	0.0513
IGF1	1.135	0.605	1	0.82	NS	0.0196	NS
CD206	0.98	0.6	1.22	0.96	NS	0.0224	NS
M2b phenotype							
IL-1RA	1.01	9.805	0.955	5.64	**0.0004**	< 0.0001	0.0004
IL-4Rα	0.995	2.2	0.975	2.18	NS	0.0181	NS
SOCS3	0.955	0.685	1.03	1	NS	NS	NS

The data shown represent median values of n = 6 mice per group. Two-way analyses of variance (ANOVAs) LPS *vs* control × ketamine *vs* placebo were performed. The "interaction" column indicates if an interaction between the condition (LPS or control) and the treatment (ketamine or placebo) could affect the results, the "condition" and "treatment" columns indicate if the condition (LPS or control) or the treatment (ketamine or placebo) could affect the results. NS: not significant. Data are represented as fold changes using the $2^{-\Delta\Delta CT}$ method.

observed for the Ptgs2 gene expression ($F(1,19) = 11.38$, $p = 0.0032$). The LPS-KET90 group presented with a significantly lower Ptgs2 gene expression than the LPS-PLACEBO group and did not differ significantly from transcript levels in the CTRL-PLACEBO group.

LPS had an impact on microglial polarization via TNF-α gene expression levels (Fig. 2d). A significant LPS *vs* control × ketamine *vs* placebo interaction was observed ($F(1,20) = 9.822$, $p = 0.0052$). The LPS-KET90 group presented with a significantly lower TNF-α expression than the LPS-PLACEBO group ($p = 0.0023$) but the expression remained higher than in the CTRL-PLACEBO group ($p = 0.0074$).

Considering the markers of the microglia M2b state, a significant LPS *vs* control × ketamine *vs* placebo interaction ($F(1,20) = 20.22$, $p = 0.0002$) was observed for IL-1RA transcripts. The LPS-KET90 group presented with a significantly lower IL-1RA gene expression than the LPS-PLACEBO group ($p < 0.0001$) but still differed significantly from transcript levels in the CTRL-PLACEBO group. No impact of ketamine on the SOCS3 or the IL-4Rα mRNA levels was observed.

Analysis of the M2a neuroprotective phenotypic markers revealed a significant LPS *vs* control × ketamine *vs* placebo interaction ($F(1,19) = 4.54$, $p = 0.0463$) for LGALS3 transcripts. The LPS-PLACEBO group presented with a significantly higher LGALS3 expression in comparison to the CTRL-PLACEBO group.

In the LPS condition, lower ketamine doses (10 mg/kg) in mice induced enhanced IGF1 gene expression, highlighting a more pronounced switch towards the M2a profile than at the dose of 90 mg/kg (Table S2). The same trends but without statistical significance on transcriptional alterations of M1 and M2b markers (Table S2) but also on TNF-α mRNA expression (Fig. S3a) were found.

3.1.3. Investigating the impact of ketamine on the cellular pathways implicated in neuroinflammation

3.1.3.1. Ketamine reversed the LPS-induced overexpression of Heme oxygenase-1 (HO-1) transcripts. We investigated the expression of HO-1, an inducible heme-degrading enzyme. HO-1 breaks down heme into carbon monoxide, free iron, and biliverdin, thereby participating in the cell defense against oxidative stress. A LPS *vs* control × ketamine *vs* placebo interaction is observed ($F(1,20) = 4.001$, $p = 0.05$). LPS alone induced a significant HO-1 gene expression in the extracted microglial cells compared to the CTRL group. This effect was reversed by treatment with ketamine: the LPS-KET90 group presented with a significantly lower HO-1 expression than the LPS-PLACEBO group (Fig. 2d), indicating a modulation and mitigation of the LPS-induced neuroinflammation by ketamine.

Within the context of LPS condition, mice treated with ketamine at 10 mg/kg presented with the same trends for HO1 mRNA expression than those treated with ketamine at the dose of 90 mg/kg (Fig. S3b).

3.1.3.2. LPS changed cerebral tryptophan catabolism through the kynurenine pathway, which was partially restored by ketamine administration. To determine the mechanism by which alterations in tryptophan degradation contribute to depressive-like behavior, we measured tryptophan (TRYP), serotonin (5HT) and their metabolites in the entire brain of mice. No LPS *vs* control × ketamine *vs* placebo interaction was observed when we took into consideration the intra-parenchymal levels of TRYP, kynurenine (KYN) and thus the KYN/TRYP ratio (Fig. 3a and b). KYN is metabolized in the brain via the kynurenine 3-monooxygenase (KMO) pathway, produced exclusively by activated microglial cells, thereby regulating the production of quinolinic acid (QUIN). A significant LPS *vs* control × ketamine *vs* placebo interaction was observed for QUIN levels ($F(1,20) = 20.56$, $p = 0.0002$). When ketamine was administered, the increase in concentration of QUIN observed in the LPS-PLACEBO group in comparison to the CTRL-PLACEBO group was reversed (Fig. 3c). Importantly, ketamine alone did not alter QUIN concentrations. No difference was observed in 5HT concentrations between the groups (Fig. 3d).

A significant LPS *vs* control × ketamine *vs* placebo interaction was determined for kynurenic acid (KYNA) levels ($F(1,20) = 30.52$, $p < 0.0001$). When ketamine was administered, the decrease in concentration of KYNA observed in the LPS-PLACEBO group in comparison to the CTRL-PLACEBO group was reversed. A significant LPS *vs* control × ketamine *vs* placebo interaction was observed for the KYNA/QUIN ratio ($F(1,20) = 36.72$, $p < 0.0001$). The LPS-PLACEBO group presented with a significantly lower ratio than the CTRL-PLACEBO group without any significant reversion induced by ketamine injection (mean difference 0.09, $p = 0.09$) (Fig. 3e). In order to define the level of the ketamine action, we measured the 3-hydroxykynurénine (3HK) parenchymal concentrations. A significant LPS *vs* control × ketamine *vs* placebo interaction was observed ($F(1,20) = 49.69$, $p < 0.0001$). The trends for the 3HK concentrations were similar to those of the QUIN concentrations. The LPS-PLACEBO group presented with a significantly higher 3HK concentration in comparison to the CTRL-PLACEBO group that was reversed by ketamine injection at the same proportions as the QUIN concentrations (Fig. 3e). It should be noted that ketamine alone alters 3HK concentrations: the CTRL-KET90 group differed from CTRL-PLACEBO group (mean difference = 2 pg/mg, $p < 0.0001$).

Again, mice in the LPS condition treated with ketamine at a sub-anesthetic dose (10 mg/kg) mirrored these effects on the KYN pathway, including for the production of QUIN (Fig. S4).

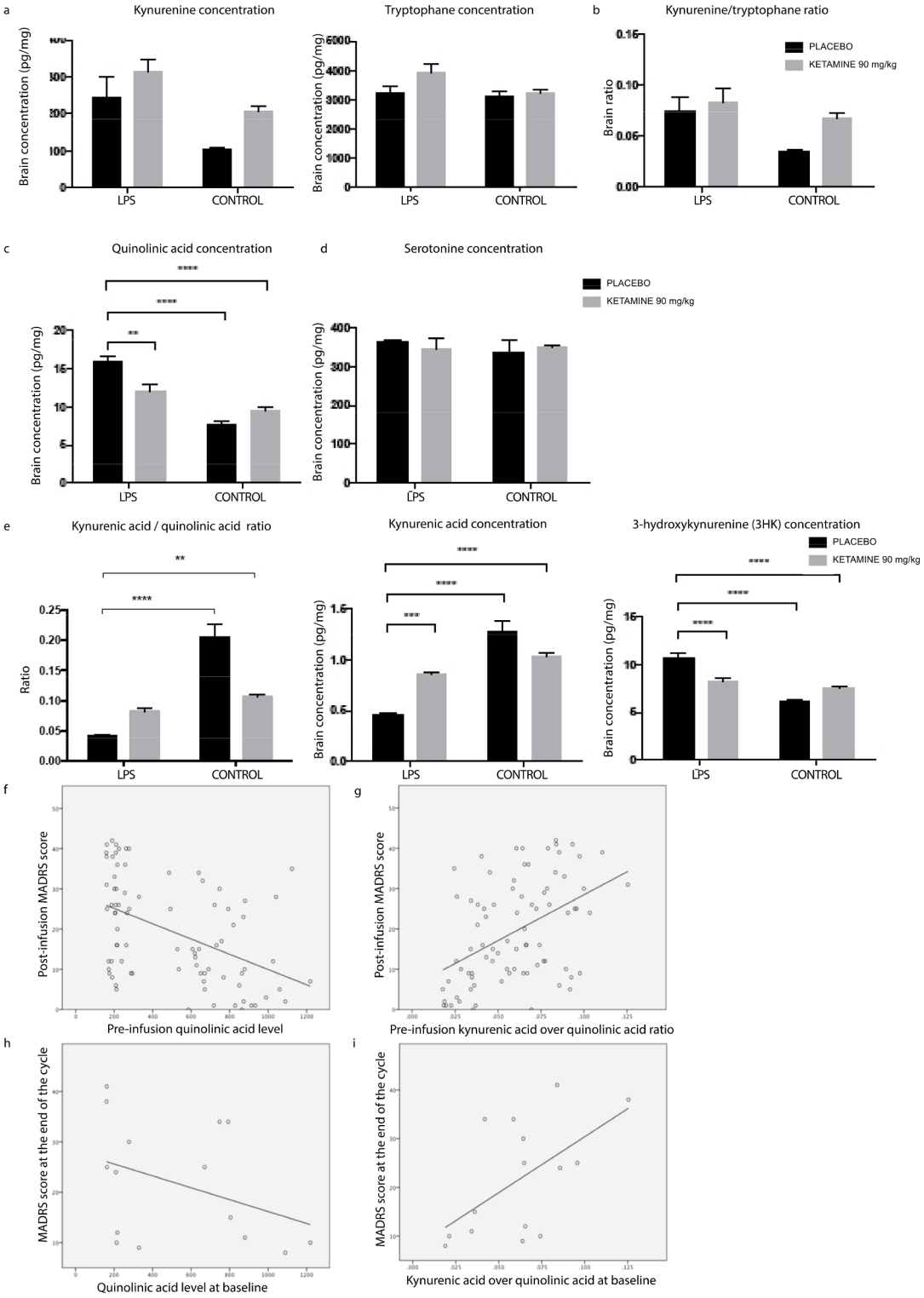


Fig. 3. Ketamine modulates tryptophan metabolism in a murine model and in patients with Treatment-Resistant Depression. (a) Kynurenine and tryptophan concentrations and (b) kynurenine/tryptophan ratio in the brain parenchyma of mice. (c) Quinolinic acid concentration. (d) Serotonin concentration. (e) Kynurenic acid/quinolinic acid ratio, kynurenic acid and 3-hydroxykynurenine (3HK) concentrations in the brain parenchyma. All data are expressed as median (± SEM) in pg/mg of cerebral tissue (n = 6 mice per group). Two-way analyses of variance (ANOVAs) (LPS *vs* NaCl × ketamine *vs* placebo) were performed. When a significant interaction was observed, planned comparisons were performed for the LPS/Placebo group against the three other groups. The significance of these planned comparisons is indicated with asterisks ($^{*}p < 0.05$, $^{**}p < 0.01$, $^{***}p < 0.001$, $^{****}p < 0.0001$). (f) Scatter graph showing the relationship between QUIN before ketamine infusion and MADRS score 24 h after infusion. Spearman's correlation $\rho = -0.46$ ($p < 0.0001$); n = 83 infusions. (g) Scatter graph showing the relationship between KYNA/QUIN before ketamine infusion and MADRS score 24 h after infusion. Pearson's correlation $r = 0.46$ ($p < 0.0001$); n = 83 infusions. (h) Scatter graph showing the relationship between baseline QUIN and final MADRS score after ketamine cycle. Pearson's correlation $r = -0.37$ ($p = 0.17$); n = 15 patients. (i) Scatter graph showing the relationship between the baseline KYNA/QUIN and the final MADRS score after ketamine cycle in patients. Pearson's correlation $r = 0.56$ ($p = 0.027$); n = 15 patients.

Table 3
Correlation coefficients between cerebral tryptophan catabolism and plasmatic tryptophan catabolism.

		Brain						
		TRYP (pg/mg)	5-HT (pg/mg)	5-HIAA (pg/mg)	KYN (pg/mg)	QUIN (pg/mg)	KYNA (pg/mg)	3HK (pg/mg)
Plasma	TRYP (μM)	−0,21	−0,40*	0,21	0,19	0,39	−0,35	0,42
	5-HT (μM)	0,26	−0,02	0,29	0,30	0,17	−0,24	0,19
	5-HIAA (nM)	0,26	0,14	0,22	0,39	0,41*	−0,33	0,19
	KYN (μM)	−0,28	**−0,61*****	0,56***	**0,86******	**0,83******	**−0,89******	**0,87******
	QUIN (nM)	−0,32	−0,36	0,49*	**0,67******	**0,71******	**−0,59******	**0,66******
	KYNA (nM)	0,23	0,51**	**−0,57*****	**−0,87******	**−0,87******	**0,81******	**−0,75******
	3HK (nM)	−0,35	−0,53**	0,36	**0,59*****	**0,61*****	**−0,70*****	**0,72******

The data shown represent Spearman coefficients between cerebral tryptophan catabolism and plasmatic tryptophan catabolism including tryptophan (TRYP), serotonin (5HT), kynurenine (KYN), 5-hydroxyindoleacetic acid (5-HIAA), 3-hydroxykynurénine (3HK) kynurenic acid (KYNA) and quinolinic acid (QUIN). The coefficients higher than 0.6 or lower than – 0.6 are in bold. The statistical significance of these coefficients is indicated with asterisks ($^{*}p < 0.05$, $^{**}p < 0.01$, $^{***}p < 0.001$, $^{****}p < 0.0001$).

3.1.3.3. Cerebral tryptophan catabolism is strongly correlated with plasmatic tryptophan catabolism. Due to the fact that QUIN and KYNA do not cross the blood-brain barrier we investigated whether plasmatic concentrations of KYNA and QUIN were correlated with parenchymal concentrations.

QUIN parenchymal concentrations are strongly correlated to QUIN and KYN plasmatic concentrations ($r = 0.83$, $p < 0.005$ and $r = 0.71$, $p < 0.005$ respectively) and anti-correlated to KYNA plasmatic concentrations ($r = -0.87$, $p < 0.005$). Conversely, KYNA parenchymal concentrations are strongly correlated to KYNA plasma concentrations ($r = 0.84$, $p < 0.005$) and anti-correlated to QUIN and KYN plasmatic concentrations ($r = -0.59$, $p < 0.005$ and $r = -0.89$, $p < 0.005$ respectively) (Table 3).

3.2. Clinical study

The socio-demographic data and clinical assessment of patients at baseline are presented in Table 4. Patients received a mean number of 6.75 (± 3.6) infusions of ketamine during a cycle. A response to treatment was observed in 8 patients (53%), 3 patients (20%) were in remission. Because of the treatment-resistance of the depressive episode, several patients received co-prescription (see Table 4 for the details of the prescribed drugs).

Table 4
Main characteristics of the study population.

	Standard	Patients (n = 15)	Controls (n = 15)	Statistical test
Socio-demographic data				
Women (nb, %)	–	11 (73%)	11 (73%)	
Age (mean, sd)	–	45.7 ± 14.3	45.7 ± 14.3	
Clinical assessment of depressive disorder				
Unipolar depressive disorder (nb, %)/bipolar disorder (nb, %)	–	11 (73.3%)/4 (26.7%)	–	
MADRS at baseline (mean, sd)	–	35.3 ± 6.1	–	
Ketamine cycle				
Nb of ketamine infusions per patient (mean, sd)	–	6.75 ± 3.6	–	
Responders (nb, %)	–	8 (53%)	–	
Remitters (nb, %)	–	3 (20%)	–	
Associated treatments				
Antidepressant drugs	–	7 (46.7%)	–	
Mood stabilizers	–	10 (66.7%)	–	
Anxiolytic/hypnotic treatments				
Antipsychotic drugs	–	7 (46.7%)	–	
Benzodiazepines		4 (26.7%)		
Hypnotics		3 (20%)		
Biology				
Tryptophan ($\mu mol.L^{-1}$)	40–60	38.1 (± 11.9)	46.76 (± 5.1)	$p = 0.02^{*}$
Kynurenine ($\mu mol.L^{-1}$)	1–3	1.7 (± 0.8)	1.7 (± 0.4)	p = 0.84
IDO activity (%)	< 5	4.6 (± 2.0)	3.6 (± 0.8)	p = 0.14
Kynurenic acid ($nmol.L^{-1}$)	30–70	24.1 (± 9.1)	51.6 (± 10.8)	$p < 0.0001^{****}$
Quinolinic acid ($nmol.L^{-1}$)	50–200	529.0 (± 371.6)	119.1 (± 36.5)	$p = 0.0008^{***}$
Kynurenic acid/Quinolinic acid	0.35–0.6	0.06 (± 0.03)	0.45 (± 0.09)	$p < 0.0001^{****}$

In the sample of depressed patients (n = 15), response to treatment was defined as a 50% decrease in MADRS score. Remission was defined as a MADRS score inferior or equal to 7. Seven patients received co-prescription of antidepressant drugs (fluoxetine n = 1, vortioxetine n = 2, mianserine n = 1, venlafaxine + mianserine n = 1, maprotiline n = 1, trimipramine n = 1). Ten patients received mood stabilizers (lithium n = 4, lamotrigine n = 2, quetiapine n = 2, lithium + quetiapine n = 1, lithium + olanzapine n = 1). Seven patients received antipsychotic drugs as anxiolytic treatment (chlorpromazine n = 4, cyamemazine n = 1, loxapine n = 2). Four patients received benzodiazepines as anxiolytic treatment (oxazepam n = 1, diazepam n = 2, prazepam n = 1). Three patients received hypnotic treatment (zolpidem n = 1, zopiclone n = 2).
The measurement of biological values in a sample of age and sex-matched healthy subjects (n = 15) is presented, as well as the standard measures for these biological values obtained in our lab. The values correspond to mean and standard deviation (mean (sd)). The Wilcoxon signed rank test was used to compare kynurenic acid levels, as it was not normally distributed in patients, and a unpaired *t*-test was used for normally distributed parameters. The significance of these comparisons is indicated with asterisks ($^{*}p < 0.05$, $^{**}p < 0.01$, $^{***}p < 0.001$, $^{****}p < 0.0001$).

3.2.1. Plasma levels of kynurenine pathway metabolites are abnormal in depressed patients

TRYP was slightly diminished in patients sample compared to control group (38.1 (± 11.9) *vs* 46.76 (± 5.1) $\mu mol.L^{-1}$, p = 0.02). KYN and IDO activity were equivalent in patients and control groups. By contrast, KYNA was substantially decreased in patients sample (24.1 (± 9.1) *vs* 51.6 (± 10.8) $nmol.L^{-1}$, p < 0.0001) and QUIN was strongly increased (529.0 (± 371.6) *vs* 119.1 (± 36.5) $nmol.L^{-1}$, p = 0.0008) compared to controls. As a consequence, KYNA/QUIN was decreased in patients group compared to controls (0.06 (± 0.03) *vs* 0.45 (± 0.09), p < 0.0001).

3.2.2. KYNA/QUIN ratio before the first infusion is a marker of ketamine response

We first investigated the difference between the evaluation before the first ketamine infusion and the final evaluation, 24 h after the final ketamine infusion (n = 15). Bivariate analysis of the parameters are presented in Table S3. The final MADRS score was not correlated to the baseline MADRS score (p = 0.65). A trend for a negative correlation between the final MADRS score and the baseline QUIN plasma level (r = −0.37, p = 0.17) was observed; none of the other correlations reached significance (KYNA: p = 0.62, TRYP: p = 0.89, and KYN p = 0.80). The KYNA/QUIN ratio was positively correlated to the final MADRS score (r = 0.57, p = 0.027) – Figs. 3f, g, h and i.

We regressed the final MADRS score against the baseline MADRS, TRYP, KYN, and KYNA/QUIN, age and sex in an identical linear model. The baseline KYNA/QUIN was the only significant predictor of the final MADRS score (beta = 1.05 ± 0.35, p = 0.016). When the baseline QUIN and KYNA were separately included in the model instead of their ratio, they both failed to reach significance (beta = −1.0 ± 0.53, p = 0.09 and beta = 0.55 ± 035, p = 0.15 for QUIN and KYNA respectively).

3.2.3. QUIN before each ketamine infusion is a biomarker of ketamine response

Assessments of depression and of biological measurements for all infusions taken together are shown in Table S3 (n = 83).

The MADRS score after a ketamine infusion (post-infusion MADRS) was positively correlated to the MADRS score before an infusion (pre-infusion MADRS, r = 0.79, p < 0.0001). Post-infusion MADRS was not correlated to pre-infusion KYN and TRYP (p = 0.47 and 0.70 respectively). Post-infusion MADRS was weakly correlated to KYNA before infusion (ρ = -0.24, p = 0.03) and negatively correlated to QUIN before infusion (ρ = -0.46, p < 0.0001). Consequently, the KYNA/QUIN ratio before infusion was correlated to the post-infusion MADRS (r = 0.46, p < 0.0001).

We regressed post-infusion MADRS against pre-infusion MADRS, TRYP, KYN, and KYNA/QUIN, age and sex in an identical linear model to ensure that pre-infusion KYNA/QUIN predicted post-infusion MADRS independently of pre-infusion MADRS. Even though pre-infusion MADRS (beta = 0.72 ± 0.07, p < 0.0001) and pre-infusion TRYP (beta = 0.14 ± 0.07, p = 0.04) were also significant, the KYNA/QUIN ratio remained a strong predictor of predicted post-infusion MADRS (beta = 0.28 ± 0.07, p = 0.0002). Moreover, when KYNA and QUIN were separately included in the model instead of their ratio, only QUIN (beta = −0.31 ± 0.08, p = 0.0003) and not KYNA (beta = −0.06 ± 0.08, p = 0.42) was significant, suggesting that QUIN was indeed the best marker of ketamine efficacy.

To better understand the parameters that may influence the change in MADRS score, we regressed the relative change in MADRS (post-infusion MADRS–pre-infusion MADRS)/pre-infusion MADRS) against the relative changes in our four biological parameters. Pre-infusion MADRS was also included in the model. Critically, the only significant predictor of a relative change in MADRS score was the relative change in QUIN (beta = 0.35 ± 0.14, p = 0.015).

4. Discussion

Numerous recent studies emphasize the potential of ketamine in the treatment of depression, whether off-label (Sanacora et al., 2017), in randomized controlled clinical trials (McGirr et al., 2015; Murrough et al., 2013) or in animal models (Autry et al., 2011; Zanos et al., 2016). Its effects are particularly rapid, extensive and last up to two weeks (Kavalali and Monteggia, 2015). The main effects of ketamine are currently explained by synaptic or extra-synaptic NMDA receptor inhibitory effects (Autry et al., 2011; Zanos and Gould, 2018) and requires AMPA receptor stimulation (Zanos et al., 2016). In this study we focused on the immunomodulatory properties of ketamine that have been experimentally suggested (Chang et al., 2009; Tan et al., 2015; Wu et al., 2008) but with conflicting results in patients (Kiraly et al., 2017). To our knowledge, we are the first to demonstrate that these immunomodulatory properties operate on microglial cells in an established model of LPS-induced depression, by reducing pro-inflammatory release in the parenchyma, by attenuating morphological changes, by inducing neuroprotective polarization and crucially by reducing quinolinic acid (QUIN) production. Moreover, QUIN plasma level was also a predictor of the response to ketamine treatment in our cohort of patients with treatment-resistant depression.

LPS injection is a well-established method to induce psychiatric symptoms in mice by immune activation: the injection performed in pregnant mice is used to model schizophrenia-like behavior in the offspring and the injection performed in adult mice is used to model depressive-like behavior (Rodrigues et al., 2018). We used this model in adult male mice as it is known to induce more severe depressive-like behaviors and more robust immune activation than other murine models of depression (Zhao et al., 2017). In this model we confirmed the behavioral advance of ketamine previously demonstrated by Walker et al. (Walker et al., 2013). The concomitant injection of LPS and ketamine was decided according to the data of Walker et al that demonstrated similar effects of ketamine injections with antidepressant-like activity when ketamine was injected at the time of LPS, or at 10–24 h after LPS (Walker et al., 2013). In our model, the concentrations of the pro-inflammatory cytokines were significantly reduced by ketamine, as described in the literature (Erickson and Banks, 2011).

However, if microglia seems to be one of the main producers of cytokines, other cells in the brain could also participate, such as astrocytes, endothelial cells or recruited NK cells (He et al., 2016). To confirm the microglial involvement, we used different approaches at morphological, phenotypic and functional levels.

Applying an innovative and precise morphological approach to our study, we found numerous microglial morphological modifications associated with the injection of LPS, in particular concerning the cytoplasm and the cell body areas that are partially restored by ketamine especially in the prefrontal cortex. This regional specificity is in line with previous clinical studies that highlighted early metabolic changes in the prefrontal region preceding and predicting response to ketamine treatment (Horacek et al., 2010; Salvadore et al., 2010). In the same way, regarding the microglial transcriptional responses to LPS, ketamine injection reduced the M1 and M2b effects of LPS without having an impact on the LPS-induced M2a polarization. These two approaches, which are complementary in understanding microglial function, lead to the conclusion that ketamine directly impacts microglial cells by inducing a neuro-protective phenotype. To further confirm the involvement of microglia, we studied the tryptophan (TRYP) metabolism pathway (Réus et al., 2015), which is mainly supported by microglia in the brain. In inflammatory conditions, it leads to the production of QUIN, which operates as a NMDA receptor agonist (Guillemin, 2012; Guillemin et al., 2005; Schurr et al., 1991). In our study we observed an increase in the KYN/TRYP ratio in the LPS-treated mice compared to the control group. This finding is consistent with clinical and experimental data in the literature (André et al., 2008; Parrott et al., 2016). This alteration was not corrected by ketamine, indicating that ketamine

does not prevent the shift toward KYN production. Furthermore, no change in the 5HT levels in the cerebral parenchyma was observed between the different groups. By contrast, we observed a net effect of ketamine in counteracting the increase in QUIN production induced by LPS. Walker and colleagues hypothesized that the antidepressant effect of ketamine could be related to the NMDA antagonism, blocking the effect of QUIN at the neuronal level (Walker et al., 2013). This hypothesis is incomplete, as we demonstrate here that ketamine acts directly on QUIN biosynthesis by decreasing its production, highlighting microglia as a key target of ketamine.

We found that the effects on microglia are evidenced after the injection of low dose of ketamine (10 mg/kg) and are lower than or equivalent to the effects observed with a higher dose (90 mg/kg). Low sub-anesthetic doses of ketamine are currently used to induce an antidepressant behavioral effect in mouse models of depression. Our results show that a sub-anesthetic dose is able to counteract the LPS-induced microglial phenotype on a cellular and molecular level in mice.

Previous studies reported that CSF and plasma levels of KYNA and QUIN are highly correlated in humans (Raison et al., 2010). In line with this CSF/plasma correlation, we highlighted in our preclinical model a strong and significant correlation between cerebral and plasmatic tryptophan catabolite levels indicating that plasmatic QUIN concentrations are a true reflection of parenchymal QUIN concentrations.

Intravenous injection or intranasal administration of low doses of ketamine (Newport et al., 2015) or esketamine (Singh et al., 2016) are also used in clinical trials to treat severely depressed patients. In our study, treatment-resistant depressed patients received a cycle of ketamine infusions at a low sub-anesthetic dose (0.5 mg/kg) resulting in a significant decrease in the MADRS score. Our results are in line with several studies reporting that KYNA/QUIN is low during depressive episodes in MDD patients and bipolar patients (Liu et al., 2018; Meier et al., 2016; Ogyu et al., 2018; Savitz et al., 2015; Wurfel et al., 2017). We showed that the baseline KYNA/QUIN predicts the MADRS score after the cycle of ketamine treatment independently of the age, sex and severity of depression. To the best of our knowledge, our study is the first to demonstrate a correlation between KYNA/QUIN and a response to antidepressant treatment. Some authors recently focused on TRYP catabolic pathway without specifically attention to QUIN and highlighted conflicting results (Allen et al., 2018; Zhou et al., 2018). In depressed patients treated with fluoxetine, no changes in kynurenine metabolites blood levels was evidenced (Mackay et al., 2009), which highlights the unique feature of ketamine treatment on kynurenine pathway and neuroinflammation. Moreover, we found that the prediction of a final MADRS score by KYNA/QUIN before ketamine infusion was mainly driven by QUIN plasma level. The high variance in QUIN and KYNA plasma levels observed in patients may be due to the different pathophysiological processes at work in these patients and is of broader amplitude that the variance due to age or sex. The high correlation already described between CSF and blood levels of KYNA and QUIN in humans (Raison et al., 2010) is in line with our preclinical data showing a high correlation in mice. Altogether, these data suggest that KYNA and QUIN blood measurements is a relevant approximation of the neuroinflammatory status in patients. These data are of particular interest for the development of ketamine as an alternative to classic antidepressant strategies, as they may enable psychiatrists to target a specific sub-population of patients, with high QUIN plasma levels at baseline, who could benefit from this treatment. Several clinical studies have suggested biomarkers for ketamine response, as IL-6 with conflicting results (Kiraly et al., 2017; Yang et al., 2015), plasma BDNF, D-serine, plasma Shank3 (Ortiz et al., 2015) and metabolites of mitochondrial β-oxidation of fatty acids (Villaseñor et al., 2014). However, our study is the first to present a translational approach providing a potential mechanism of action for ketamine response and suggesting that similar pathophysiological mechanisms may be present in a mouse model and in at least a certain group of depressed patients. However, given the limited number of patients included and the absence of a two-arms (ketamine *vs* placebo) design, further clinical studies with larger sample sizes are needed to confirm our clinical results.

In conclusion, our results demonstrate that ketamine targets microglial cells in a neuroinflammatory context, proving the hypothesis of microglial involvement in the pathophysiology of depression. They pave the way for the use of quinolinic acid as a biomarker of the antidepressant effect of ketamine.

Funding

This work was supported by the Fondation des Gueules Cassées, the Comité d'Interface SFAR (Société Française d'Anesthésie-Réanimation), SRLF (Société de Réanimation de Langue Française), INSERM, the Pierre Deniker and the « entreprendre pour aider » foundations. Franck Verdonk received financial support from ANRT (Association Nationale de la Recherche et de la Technologie) through an Air Liquide-CIFRE contract 2012/1315. The Imagopole is part of the France BioImaging infrastructure supported by the French National Research Agency (ANR-10-INSB-04-01, "Investments for the future") and is grateful for the support from the Conseil de la Region Ile-de-France (program Sesame 2007, project Imagopole, S.L. Shorte).

Declaration of Competing Interest

RG has received compensation as a member of the scientific advisory board of Janssen, Lundbeck, Roche, SOBI, Takeda. He has served as a consultant and/or a speaker for Astra Zeneca, Boehringer-Ingelheim, Pierre Fabre, Lilly, Lundbeck, LVMH, MAPREG, Otsuka, Pileje, SANOFI, Servier and received compensation, and he has received research support from Servier.

FVi has been invited to scientific meetings, consulted and/or served as speaker and received compensation by Lundbeck, Servier, Recordati, Janssen, and Otsuka.

None of these links of interest are related to this work.

The remaining authors have nothing to disclose.

Acknowledgments

The authors thank Jean-Marc Cavaillon, Pierre Rocheteau, Alexandre Salvador and Denis David for their advice and comments on the manuscript. The authors also thank Patricia Flamant, Mathilde Vinet, Lucile Boccara and David Briand for their technical help, Cecile Baldassari and all the clinical teams of the Service Hospitalo-Universitaire of Hôpital Sainte Anne – Paris for their support of this research.

Appendix A. Supplementary data

Supplementary data to this article can be found online at https://doi.org/10.1016/j.bbi.2019.06.033.

References

Allen, A.P., Naughton, M., Dowling, J., Walsh, A., O'Shea, R., Shorten, G., Scott, L., McLoughlin, D.M., Cryan, J.F., Clarke, G., Dinan, T.G., 2018. Kynurenine pathway metabolism and the neurobiology of treatment-resistant depression: comparison of multiple ketamine infusions and electroconvulsive therapy. J. Psychiatr. Res. 100, 24–32. https://doi.org/10.1016/j.jpsychires.2018.02.011.

André, C., O'Connor, J.C., Kelley, K.W., Lestage, J., Dantzer, R., Castanon, N., 2008. Spatio-temporal differences in the profile of murine brain expression of proinflammatory cytokines and indoleamine 2,3-dioxygenase in response to peripheral lipopolysaccharide administration. J. Neuroimmunol. 200, 90–99.

Autry, A.E., Adachi, M., Nosyreva, E., Na, E.S., Los, M.F., Cheng, P., Kavalali, E.T., Monteggia, L.M., 2011. NMDA receptor blockade at rest triggers rapid behavioural antidepressant responses. Nature 475, 91–95. https://doi.org/10.1038/nature10130.

Beilin, B., Rusabrov, Y., Shapira, Y., Roytblat, L., Greemberg, L., Yardeni, I.Z., Bessler, H., 2007. Low-dose ketamine affects immune responses in humans during the early postoperative period. Br. J. Anaesth. 99, 522–527. https://doi.org/10.1093/bja/aem218.

Berman, R.M., Cappiello, A., Anand, A., Oren, D.A., Heninger, G.R., Charney, D.S., Krystal, J.H., 2000. Antidepressant effects of ketamine in depressed patients. Biol. Psychiatry 47, 351–354.

Bonaccorso, S., Marino, V., Puzella, A., Pasquini, M., Biondi, M., Artini, M., Almerighi, C., Verkerk, R., Meltzer, H., Maes, M., 2002. Increased depressive ratings in patients with hepatitis C receiving interferon-alpha-based immunotherapy are related to interferon-alpha-induced changes in the serotonergic system. J. Clin. Psychopharmacol. 22, 86–90.

Capuron, L., Gumnick, J.F., Musselman, D.L., Lawson, D.H., Reemsnyder, A., Nemeroff, C.B., Miller, A.H., 2002. Neurobehavioral effects of interferon-alpha in cancer patients: phenomenology and paroxetine responsiveness of symptom dimensions. Neuropsychopharmacol. Off. Publ. Am. Coll. Neuropsychopharmacol. 26, 643–652. https://doi.org/10.1016/S0893-133X(01)00407-9.

Chang, Y., Lee, J.-J., Hsieh, C.-Y., Hsiao, G., Chou, D.-S., Sheu, J.-R., 2009. Inhibitory effects of ketamine on lipopolysaccharide-induced microglial activation. Mediators Inflamm. 2009, 1–7. https://doi.org/10.1155/2009/705379.

Chhor, V., Le Charpentier, T., Lebon, S., Oré, M.-V., Celador, I.L., Josserand, J., Degos, V., Jacotot, E., Hagberg, H., Sävman, K., Mallard, C., Gressens, P., Fleiss, B., 2013. Characterization of phenotype markers and neuronotoxic potential of polarised primary microglia in vitro. Brain. Behav. Immun. 32, 70–85. https://doi.org/10.1016/j.bbi.2013.02.005.

Colton, C.A., 2009. Heterogeneity of microglial activation in the innate immune response in the brain. J. Neuroimmune Pharmacol. Off. J. Soc. NeuroImmune Pharmacol. 4, 399–418. https://doi.org/10.1007/s11481-009-9164-4.

Dantzer, R., O'Connor, J.C., Lawson, M.A., Kelley, K.W., 2011. Inflammation-associated depression: from serotonin to kynurenine. Psychoneuroendocrinology 36, 426–436. https://doi.org/10.1016/j.psyneuen.2010.09.012.

David, D.J., Samuels, B.A., Rainer, Q., Wang, J.-W., Marsteller, D., Mendez, I., Drew, M., Craig, D.A., Guiard, B.P., Guilloux, J.-P., Artymyshyn, R.P., Gardier, A.M., Gerald, C., Antonijevic, I.A., Leonardo, E.D., Hen, R., 2009. Neurogenesis-dependent and -independent effects of fluoxetine in an animal model of anxiety/depression. Neuron 62, 479–493. https://doi.org/10.1016/j.neuron.2009.04.017.

Duman, R.S., Li, N., Liu, R.-J., Duric, V., Aghajanian, G., 2012. Signaling pathways underlying the rapid antidepressant actions of ketamine. Neuropharmacology 62, 35–41. https://doi.org/10.1016/j.neuropharm.2011.08.044.

Erickson, M.A., Banks, W.A., 2011. Cytokine and chemokine responses in serum and brain after single and repeated injections of lipopolysaccharide: multiplex quantification with path analysis. Brain. Behav. Immun. 25, 1637–1648. https://doi.org/10.1016/j.bbi.2011.06.006.

Fujigaki, S., Takemura, M., Hamakawa, H., Seishima, M., Saito, K., 2003. The mechanism of interferon-gamma induced anti Toxoplasma gondii by indoleamine 2,3-dioxygenase and/or inducible nitric oxide synthase vary among tissues. Adv. Exp. Med. Biol. 527, 97–103.

Guillemin, G.J., 2012. Quinolinic acid, the inescapable neurotoxin. FEBS J. 279, 1356–1365. https://doi.org/10.1111/j.1742-4658.2012.08485.x.

Guillemin, G.J., Smythe, G., Takikawa, O., Brew, B.J., 2005. Expression of indoleamine 2,3-dioxygenase and production of quinolinic acid by human microglia, astrocytes, and neurons. Glia 49, 15–23. https://doi.org/10.1002/glia.20090.

He, H., Geng, T., Chen, P., Wang, M., Hu, J., Kang, L., Song, W., Tang, H., 2016. NK cells promote neutrophil recruitment in the brain during sepsis-induced neuroinflammation. Sci. Rep. 6, 27711. https://doi.org/10.1038/srep27711.

Horacek, J., Brunovsky, M., Novak, T., Tislerova, B., Palenicek, T., Bubenikova-Valesova, V., Spaniel, F., Koprivova, J., Mohr, P., Balikova, M., Hoschl, C., 2010. Subanesthetic dose of ketamine decreases prefrontal theta cordance in healthy volunteers: implications for antidepressant effect. Psychol. Med. 40, 1443–1451. https://doi.org/10.1017/S0033291709991619.

Jung, S., Aliberti, J., Graemmel, P., Sunshine, M.J., Kreutzberg, G.W., Sher, A., Littman, D.R., 2000. Analysis of fractalkine receptor CX(3)CR1 function by targeted deletion and green fluorescent protein reporter gene insertion. Mol. Cell. Biol. 20, 4106–4114.

Kappelmann, N., Lewis, G., Dantzer, R., Jones, P.B., Khandaker, G.M., 2018. Antidepressant activity of anti-cytokine treatment: a systematic review and meta-analysis of clinical trials of chronic inflammatory conditions. Mol. Psychiatry 23, 335–343. https://doi.org/10.1038/mp.2016.167.

Kavalali, E.T., Monteggia, L.M., 2015. How does ketamine elicit a rapid antidepressant response? Curr. Opin. Pharmacol. 20, 35–39. https://doi.org/10.1016/j.coph.2014.11.005.

Kiecolt-Glaser, J.K., Derry, H.M., Fagundes, C.P., 2015. Inflammation: depression fans the flames and feasts on the heat. Am. J. Psychiatry 172, 1075–1091. https://doi.org/10.1176/appi.ajp.2015.15020152.

Kiraly, D.D., Horn, S.R., Van Dam, N.T., Costi, S., Schwartz, J., Kim-Schulze, S., Patel, M., Hodes, G.E., Russo, S.J., Merad, M., Iosifescu, D.V., Charney, D.S., Murrough, J.W., 2017. Altered peripheral immune profiles in treatment-resistant depression: response to ketamine and prediction of treatment outcome. Transl. Psychiatry 7, e1065. https://doi.org/10.1038/tp.2017.31.

Langlieb, A.M., Guico-Pabia, C.J., 2010. Beyond symptomatic improvement: assessing real-world outcomes in patients with major depressive disorder. Prim. Care Companion J. Clin. Psychiatry 12. https://doi.org/10.4088/PCC.09r00826blu.

Liu, H., Ding, L., Zhang, H., Mellor, D., Wu, H., Zhao, D., Wu, C., Lin, Z., Yuan, J., Peng, D., 2018. The metabolic factor kynurenic acid of kynurenine pathway predicts major depressive disorder. Front. Psychiatry 9. https://doi.org/10.3389/fpsyt.2018.00552.

Ma, Z., Zang, T., Birnbaum, S.G., Wang, Z., Johnson, J.E., Zhang, C.-L., Parada, L.F., 2017. TrkB dependent adult hippocampal progenitor differentiation mediates sustained ketamine antidepressant response. Nat. Commun. 8, 1668. https://doi.org/10.1038/s41467-017-01709-8.

Mackay, G.M., Forrest, C.M., Christofides, J., Bridel, M.A., Mitchell, S., Cowlard, R., Stone, T.W., Darlington, L.G., 2009. Kynurenine metabolites and inflammation markers in depressed patients treated with fluoxetine or counselling. Clin. Exp. Pharmacol. Physiol. 36, 425–435. https://doi.org/10.1111/j.1440-1681.2008.05077.x.

Maes, M., 1999. Major depression and activation of the inflammatory response system. Adv. Exp. Med. Biol. 461, 25–46. https://doi.org/10.1007/978-0-585-37970-8_2.

Mantovani, A., Sica, A., Sozzani, S., Allavena, P., Vecchi, A., Locati, M., 2004. The chemokine system in diverse forms of macrophage activation and polarization. Trends Immunol. 25, 677–686. https://doi.org/10.1016/j.it.2004.09.015.

McGirr, A., Berlim, M.T., Bond, D.J., Fleck, M.P., Yatham, L.N., Lam, R.W., 2015. A systematic review and meta-analysis of randomized, double-blind, placebo-controlled trials of ketamine in the rapid treatment of major depressive episodes. Psychol. Med. 45, 693–704. https://doi.org/10.1017/S0033291714001603.

Meier, T.B., Drevets, W.C., Wurfel, B.E., Ford, B.N., Morris, H.M., Victor, T.A., Bodurka, J., Teague, T.K., Dantzer, R., Savitz, J., 2016. Relationship between neurotoxic kynurenine metabolites and reductions in right medial prefrontal cortical thickness in major depressive disorder. Brain. Behav. Immun. 53, 39–48. https://doi.org/10.1016/j.bbi.2015.11.003.

Mendez-David, I., David, D.J., Darcet, F., Wu, M.V., Kerdine-Römer, S., Gardier, A.M., Hen, R., 2014. Rapid anxiolytic effects of a 5-HT_4 receptor agonist are mediated by a neurogenesis-independent mechanism. Neuropsychopharmacol. Off. Publ. Am. Coll. Neuropsychopharmacol. 39, 1366–1378. https://doi.org/10.1038/npp.2013.332.

Miller, A.H., Maletic, V., Raison, C.L., 2009. Inflammation and its discontents: the role of cytokines in the pathophysiology of major depression. Biol. Psychiatry, Social Stresses and Depression 65, 732–741. https://doi.org/10.1016/j.biopsych.2008.11.029.

Murrough, J.W., Iosifescu, D.V., Chang, L.C., Al Jurdi, R.K., Green, C.E., Perez, A.M., Iqbal, S., Pillemer, S., Foulkes, A., Shah, A., Charney, D.S., Mathew, S.J., 2013. Antidepressant efficacy of ketamine in treatment-resistant major depression: a two-site randomized controlled trial. Am. J. Psychiatry 170, 1134–1142. https://doi.org/10.1176/appi.ajp.2013.13030392.

Newport, D.J., Carpenter, L.L., McDonald, W.M., Potash, J.B., Tohen, M., Nemeroff, C.B., APA Council of Research Task Force on Novel Biomarkers and Treatments, 2015. Ketamine and other NMDA antagonists: early clinical trials and possible mechanisms in depression. Am. J. Psychiatry 172, 950–966. https://doi.org/10.1176/appi.ajp.2015.15040465.

O'Connor, J.C., Lawson, M.A., André, C., Moreau, M., Lestage, J., Castanon, N., Kelley, K.W., Dantzer, R., 2009. Lipopolysaccharide-induced depressive-like behavior is mediated by indoleamine 2,3-dioxygenase activation in mice. Mol. Psychiatry 14, 511–522. https://doi.org/10.1038/sj.mp.4002148.

Ogyu, K., Kubo, K., Noda, Y., Iwata, Y., Tsugawa, S., Omura, Y., Wada, M., Tarumi, R., Plitman, E., Moriguchi, S., Miyazaki, T., Uchida, H., Graff-Guerrero, A., Mimura, M., Nakajima, S., 2018. Kynurenine pathway in depression: a systematic review and meta-analysis. Neurosci. Biobehav. Rev. 90, 16–25. https://doi.org/10.1016/j.neubiorev.2018.03.023.

Ortiz, R., Niciu, M.J., Lukkahati, N., Saligan, L.N., Nugent, A.C., Luckenbaugh, D.A., Machado-Vieira, R., Zarate, C.A., 2015. Shank3 as a potential biomarker of antidepressant response to ketamine and its neural correlates in bipolar depression. J. Affect. Disord. 172, 307–311. https://doi.org/10.1016/j.jad.2014.09.015.

Parrott, J.M., Redus, L., Santana-Coelho, D., Morales, J., Gao, X., O'Connor, J.C., 2016. Neurotoxic kynurenine metabolism is increased in the dorsal hippocampus and drives distinct depressive behaviors during inflammation. e918–e918. Transl. Psychiatry 6. https://doi.org/10.1038/tp.2016.200.

Pham, T.H., Mendez-David, I., Defaix, C., Guiard, B.P., Tritschler, L., David, D.J., Gardier, A.M., 2017. Ketamine treatment involves medial prefrontal cortex serotonin to induce a rapid antidepressant-like activity in BALB/cJ mice. Neuropharmacology 112, 198–209. https://doi.org/10.1016/j.neuropharm.2016.05.010.

Raison, C.L., Dantzer, R., Kelley, K.W., Lawson, M.A., Woolwine, B.J., Vogt, G., Spivey, J.R., Saito, K., Miller, A.H., 2010. CSF concentrations of brain tryptophan and kynurenines during immune stimulation with IFN-α: relationship to CNS immune responses and depression. Mol. Psychiatry 15, 393–403. https://doi.org/10.1038/mp.2009.116.

Raison, C.L., Rutherford, R.E., Woolwine, B.J., Shuo, C., Schettler, P., Drake, D.F., Haroon, E., Miller, A.H., 2013. A randomized controlled trial of the tumor necrosis factor antagonist infliximab for treatment-resistant depression: the role of baseline inflammatory biomarkers. JAMA Psychiatry 70, 31–41. https://doi.org/10.1001/2013.jamapsychiatry.4.

Ramaker, M.J., Dulawa, S.C., 2017. Identifying fast-onset antidepressants using rodent models. Mol. Psychiatry 22, 656–665. https://doi.org/10.1038/mp.2017.36.

Ransohoff, R.M., Perry, V.H., 2009. Microglial physiology: unique stimuli, specialized responses. Annu. Rev. Immunol. 27, 119–145. https://doi.org/10.1146/annurev.immunol.021908.132528.

Réus, G.Z., Jansen, K., Titus, S., Carvalho, A.F., Gabbay, V., Quevedo, J., 2015. Kynurenine pathway dysfunction in the pathophysiology and treatment of depression: evidences from animal and human studies. J. Psychiatr. Res. 68, 316–328. https://doi.org/10.1016/j.jpsychires.2015.05.007.

Rodrigues, F.T.S., de Souza, M.R.M., Lima, C.N. de C., da Silva, F.E.R., Costa, D.V. da S., dos Santos, C.C., Miyajima, F., de Sousa, F.C.F., Vasconcelos, S.M.M., Barichello, T., Quevedo, J., Maes, M., de Lucena, D.F., Macedo, D., 2018. Major depression model induced by repeated and intermittent lipopolysaccharide administration: long-lasting behavioral, neuroimmune and neuroprogressive alterations. J. Psychiatr. Res. 107, 57–67. https://doi.org/10.1016/j.jpsychires.2018.10.003.

Salvadore, G., Cornwell, B.R., Sambataro, F., Latov, D., Colon-Rosario, V., Carver, F., Holroyd, T., DiazGranados, N., Machado-Vieira, R., Grillon, C., Drevets, W.C., Zarate, C.A., 2010. Anterior cingulate desynchronization and functional connectivity with the amygdala during a working memory task predict rapid antidepressant response to ketamine. Neuropsychopharmacology 35, 1415–1422. https://doi.org/10.1038/npp.

2010.24.
Sanacora, G., Frye, M.A., McDonald, W., Mathew, S.J., Turner, M.S., Schatzberg, A.F., Summergrad, P., Nemeroff, C.B., American Psychiatric Association (APA) Council of Research Task Force on Novel Biomarkers and Treatments, 2017. A consensus statement on the use of ketamine in the treatment of mood disorders. JAMA Psychiatry 74, 399. https://doi.org/10.1001/jamapsychiatry.2017.0080.
Savitz, J., Drevets, W.C., Wurfel, B.E., Ford, B.N., Bellgowan, P.S.F., Victor, T.A., Bodurka, J., Teague, T.K., Dantzer, R., 2015. Reduction of kynurenic acid to quinolinic acid ratio in both the depressed and remitted phases of major depressive disorder. Brain Behav. Immun. 46, 55–59. https://doi.org/10.1016/j.bbi.2015.02.007.
Schmittgen, T.D., Livak, K.J., 2008. Analyzing real-time PCR data by the comparative C(T) method. Nat. Protoc. 3, 1101–1108.
Schurr, A., West, C.A., Rigor, B.M., 1991. Neurotoxicity of quinolinic acid and its derivatives in hypoxic rat hippocampal slices. Brain Res. 568, 199–204.
Singh, J.B., Fedgchin, M., Daly, E., Xi, L., Melman, C., De Bruecker, G., Tadic, A., Sienaert, P., Wiegand, F., Manji, H., Drevets, W.C., Van Nueten, L., 2016. Intravenous esketamine in adult treatment-resistant depression: a double-blind, double-randomization, placebo-controlled study. Biol. Psychiatry 80, 424–431. https://doi.org/10.1016/j.biopsych.2015.10.018.
Sinyor, M., Schaffer, A., Levitt, A., 2010. The sequenced treatment alternatives to relieve depression (STAR*D) trial: a review. Can. J. Psychiatry. 55, 126–135.
Steiner, J., Walter, M., Gos, T., Guillemin, G.J., Bernstein, H.-G., Sarnyai, Z., Mawrin, C., Brisch, R., Bielau, H., zu Schwabedissen, L., Bogerts, B., Myint, A.-M., 2011. Severe depression is associated with increased microglial quinolinic acid in subregions of the anterior cingulate gyrus: evidence for an immune-modulated glutamatergic neurotransmission? J. Neuroinflamm. 8, 94. https://doi.org/10.1186/1742-2094-8-94.
Takahashi, T., Kinoshita, M., Shono, S., Habu, Y., Ogura, T., Seki, S., Kazama, T., 2010. The effect of ketamine anesthesia on the immune function of mice with postoperative septicemia. Anesth. Analg. 111, 1. https://doi.org/10.1213/ANE.0b013e3181ed12fc.
Tan, Y., Wang, Q., She, Y., Bi, X., Zhao, B., 2015. Ketamine reduces LPS-induced HMGB1 via activation of the Nrf2/HO-1 pathway and NF-κB suppression. J. Trauma Acute Care Surg. 78, 784–792. https://doi.org/10.1097/TA.0000000000000588.
Verdonk, F., Roux, P., Flamant, P., Fiette, L., Bozza, F.A., Simard, S., Lemaire, M., Plaud, B., Shorte, S.L., Sharshar, T., Chrétien, F., Danckaert, A., 2016. Phenotypic clustering: a novel method for microglial morphology analysis. J. Neuroinflamm. 13, 153. https://doi.org/10.1186/s12974-016-0614-7.
Villaseñor, A., Ramamoorthy, A., Silva dos Santos, M., Lorenzo, M.P., Laje, G., Zarate, C., Barbas, C., Wainer, I.W., 2014. A pilot study of plasma metabolomic patterns from patients treated with ketamine for bipolar depression: evidence for a response-related difference in mitochondrial networks. Br. J. Pharmacol. 171, 2230–2242. https://doi.org/10.1111/bph.12494.
Walker, A.K., Budac, D.P., Bisulco, S., Lee, A.W., Smith, R.A., Beenders, B., Kelley, K.W., Dantzer, R., 2013. NMDA receptor blockade by ketamine abrogates lipopolysaccharide-induced depressive-like behavior in C57BL/6J mice. Neuropsychopharmacology 38, 1609–1616. https://doi.org/10.1038/npp.2013.71.
Wu, G.-J., Chen, T.-L., Ueng, Y.-F., Chen, R.-M., 2008. Ketamine inhibits tumor necrosis factor-α and interleukin-6 gene expressions in lipopolysaccharide-stimulated macrophages through suppression of toll-like receptor 4-mediated c-Jun N-terminal kinase phosphorylation and activator protein-1 activation. Toxicol. Appl. Pharmacol. 228, 105–113. https://doi.org/10.1016/j.taap.2007.11.027.
Wurfel, B.E., Drevets, W.C., Bliss, S.A., McMillin, J.R., Suzuki, H., Ford, B.N., Morris, H.M., Teague, T.K., Dantzer, R., Savitz, J.B., 2017. Serum kynurenic acid is reduced in affective psychosis. Transl. Psychiatry 7, e1115. https://doi.org/10.1038/tp.2017.88.
Yang, J.-J., Wang, N., Yang, C., Shi, J.-Y., Yu, H.-Y., Hashimoto, K., 2015. Serum interleukin-6 is a predictive biomarker for ketamine's antidepressant effect in treatment-resistant patients with major depression. Biol. Psychiatry 77, e19–e20. https://doi.org/10.1016/j.biopsych.2014.06.021.
Yirmiya, R., Rimmerman, N., Reshef, R., 2015. Depression as a microglial disease. Trends Neurosci. 38, 637–658. https://doi.org/10.1016/j.tins.2015.08.001.
Zanos, P., Gould, T.D., 2018. Mechanisms of ketamine action as an antidepressant. Mol. Psychiatry 23, 801–811. https://doi.org/10.1038/mp.2017.255.
Zanos, P., Moaddel, R., Morris, P.J., Georgiou, P., Fischell, J., Elmer, G.I., Alkondon, M., Yuan, P., Pribut, H.J., Singh, N.S., Dossou, K.S.S., Fang, Y., Huang, X.-P., Mayo, C.L., Wainer, I.W., Albuquerque, E.X., Thompson, S.M., Thomas, C.J., Zarate, C.A., Gould, T.D., 2016. NMDAR inhibition-independent antidepressant actions of ketamine metabolites. Nature 533, 481–486. https://doi.org/10.1038/nature17998.
Zarate, C.A., Singh, J.B., Carlson, P.J., Brutsche, N.E., Ameli, R., Luckenbaugh, D.A., Charney, D.S., Manji, H.K., 2006. A randomized trial of an N-methyl-D-aspartate antagonist in treatment-resistant major depression. Arch. Gen. Psychiatry 63, 856. https://doi.org/10.1001/archpsyc.63.8.856.
Zhao, X., Cao, F., Liu, Q., Li, X., Xu, G., Liu, G., Zhang, Y., Yang, X., Yi, S., Xu, F., Fan, K., Ma, J., 2017. Behavioral, inflammatory and neurochemical disturbances in LPS and UCMS-induced mouse models of depression. Behav. Brain Res. https://doi.org/10.1016/j.bbr.2017.05.064.
Zhou, Y., Zheng, W., Liu, W., Wang, C., Zhan, Y., Li, H., Chen, L., Li, M., Ning, Y., 2018. Antidepressant effect of repeated ketamine administration on kynurenine pathway metabolites in patients with unipolar and bipolar depression. Brain. Behav. Immun. 74, 205–212. https://doi.org/10.1016/j.bbi.2018.09.007.